DOE/PC/92534--T4

SELECTIVE CATALYTIC REDUCTION OF SULFUR DIOXIDE TO ELEMENTAL SULFUR

Quarterly Technical Progress Report No. 6

October - December 1993

Wei Liu
Maria Flytzani-Stephanopoulos
Adel F. Sarofim

Department of Chemical Engineering
Massachusetts Institute of Technology
Cambridge, MA 02139

DISCLAIMER

This report was prepared as an account of work sponsored by an agency of the United States Government. Neither the United States Government nor any agency thereof, nor any of their employees, makes any warranty, express or implied, or assumes any legal liability or responsibility for the accuracy, completeness, or usefulness of any information, apparatus, product, or process disclosed, or represents that its use would not infringe privately owned rights. Reference herein to any specific commercial product, process, or service by trade name, trademark, manufacturer, or otherwise does not necessarily constitute or imply its endorsement, recommendation, or favoring by the United States Government or any agency thereof. The views and opinions of authors expressed herein do not necessarily state or reflect those of the United States Government or any agency thereof.

Prepared for
The U.S. Department of Energy
The Pittsburgh Energy Technology Center
Pittsburgh, Pennsylvania
Technical Project Officer: Dr. Richard Tischer
Grant No.: DE-FG22-92PC92534

US/DOE Patent Clearance is not required prior to the publication of this document

ACQUISITION & ASSISTANCE DIV.
94 FEB -4 PM 2:38
RECEIVED
USDOE/PETC

MASTER

DISTRIBUTION OF THIS DOCUMENT IS UNLIMITED

ABSTRACT

Elemental sulfur recovery from SO_2-containing gas stream is highly attractive as it produces a salable product and no waste to dispose of. However, commercially available schemes are complex and involve multi-stage reactors, such as , most notably in the Resox (reduction of SO_2 with coke) and Claus plant(reaction of SO_2 with H_2S over catalyst). This project will investigate a cerium oxide catalyst for the single stage selective reduction of SO_2 to elemental sulfur by a reductant, such as carbon monoxide. Cerium oxide has been identified in recent work at MIT as a superior catalyst for SO_2 reduction by CO to elemental sulfur because its high activity and high selectivity to sulfur over COS over a wide temperature range(400-650 ^oC). The detailed kinetic and parametric studies of SO_2 reduction planned in this work over various CeO_2-formulations will provide the necessary basis for development of a very simplified process, namely that of a single-stage elemental sulfur recovery scheme from variable concentration gas streams, The potential cost- and energy-efficiency benefits from this approach can not be overstated. A first apparent application is treatment of a regenerator off-gases in power plants using regenerative flue gas desulfurization. Such a simple catalytic converter may offer the long-sought "Claus-alternative" for coal-fired power plant applications.

PROGRESS SUMMARY

Last quarter we reported that transition metal-doped fluorite oxides are active catalysts for sulfur dioxide reduction. Systematic examination of the Ce-Cu-O catalyst system identified the catalyst containing about 15 at% copper as the most active and stable. In this quarter the Cu-Ce-O catalyst was characterized by several analytical techniques to understand the relationship between catalytic properties and catalyst structure and composition.

X-ray Powder Diffraction(XRD) Analysis

XRD was performed on a Rigaku RU300 X-ray diffractometer using Cu K α radiation. The X-ray tube was operated at 200 mA and 50 kV. A diverging slit of 1°, scattering slit of 1°, and receiving slit 0.15^o were used. In the XRD phase composition survey, a scan rate of 10°/min was used while in the lattice parameter measurement 1°/min was used. XRD analyses of the Cu-Ce-O system identified two crystal phases, fluorite-type and copper oxide, in catalysts containing over 20 at% copper, and only the fluorite structure in the composites containing less than 20 at % Cu. Also in the Y-doped and Cu-doped zirconia catalysts, only the fluorite-type structure was found. Two small peaks due to CuO phase were found in the fresh 3.7at% Cu/CeO_2 catalysts as shown in Figure 1, but, these two peaks disappeared after use in reduction of sulfur dioxide. The distinct fluorite-type diffraction pattern was found in both the used and fresh Cu-Ce-O catalysts, which indicates that the fluorite oxide was stable in the present reaction conditions.

Figure 2 shows the variance of lattice space with copper content in the $Cu_xCe_{1-x}(La)O_{2-x}$. The lattice parameter of ceria FCC crystal structure was calculated with standard formula $2D_{hkl}\sin\theta=n\lambda$($\lambda$=0.15405 nm for Cu K$\alpha$1) using the (111) diffraction line which is the strongest line and also contains the

least interference from Cu Kα2 radiation. The data plotted in Figure 2 can be roughly correlated with a linear equation which suggests the formation of a solid solution according to Vegard's rule. The lattice parameters for both fresh and used x=0.15 catalysts strongly deviate from the straight line. The unit cell of the x=0.15 sample is equal to the $Ce(La)O_2$, suggesting no solid solution formation. The fact that the x=0.15 catalyst was identified as the most active catalyst then suggests that solid solution formation may not improve the catalytic activity. The stability of the solid solution Cu-Ce-O was tested by calcining x =0.15 and 0.25 samples for 17 hours at 750 ^{o}C in air. Relatively small CuO peaks were found in the XRD diagrams of both catalysts. As shown in Figure 2, their lattice parameters were also changed to a same value. It seems that a solubility limit was reached.

Scanning Transmission Electron Microscopy(STEM) Analysis

STEM analyses were performed on a Vacuum Generators HB-5 and HB603 apparatus which provides high spatial resolution for both imaging and compositional analysis. To do this experiment, finely grounded catalyst powder was embedded in a resin matrix. Then, the matrix was ultramicrotomed to slices of 80 to 120 nm. STEM analyses of the fresh Cu-Ce-O composite catalyst found the copper as small particles(a few nm) and large agglomerates(>10 nm), the latter increasing in population with the copper content. Figure 3 is the elemental map on a used x=0.2 catalyst. Extensive copper coverage and association with sulfur was observed. The copper particle size varies from a few to a few hundred nanometer. In contrast, a higher number and uniform dispersion of small copper particles(a few nm) was found on the used x=0.15 catalyst as shown in Figure 4. This may explain why the x=0.15 catalyst was much more active than the x=0.2 though there is not much difference in elemental composition. Figure 5 shows

the elemental mapping for the Cu/CeO_2 before and after use. In Figure 5, the left-hand-side top and bottom pictures are the dark field images of the fresh catalyst matrix and the bright field image of the used one, respectively, while the right-hand-side pictures are the corresponding elemental mapping images. The rulers are applied to the elemental maps. Many large copper particles(~300 nm) were found in the fresh catalyst, but relatively smaller particles on the used one. Sulfur found on the used catalyst was also associated with copper. It is interesting that the copper became more finely dispersed in the used catalyst. This result confirms the CuO peak disappearance in the XRD diagram of the used Cu/CeO_2 catalyst.

X-ray Photoelectron Spectroscopy(XPS) Analysis

XPS analysis on the catalyst surface was performed on a Perkin Elmer 5100 Model instrument equipped with a Argon ion gun. Mg X-ray source of 1253.6eV was used with the power set at 15 kV and 300 W. Catalyst powder sample was pressed on a indium plate and transferred to the vacuum chamber without any pretreatment. Data was acquired under vacuum about 10^{-9} torr. Figure 6 shows the XPS survey of the fresh x=0.15 catalyst. Comparison with the standard spectra[1] finds the Cu_{2p} satellite similar to the reduced copper(Cu, Cu^{+1}) and Ce_{3d} satellite for both fresh and used catalysts similar to bulk ceria. In other experiments, the Cu_{2p} XPS of the $CuO/\gamma\text{-}Al_2O_3$ looked exactly like that of CuO, but, the Cu_{2p} XPS of the $CuOx/CeO_2$ is between the CuO and reduced CuO(Cu, Cu^{+1}). The binding energies of the $Cu_{0.15}Ce_{0.85}(La)O_x$ catalyst found by using ESCA MULTIPLEX with total 90 min acquisition time are summarized in Table 1. Hydrocarbon-type carbon peak was found in all the samples which may be inadvertently contaminated. Thus, all the binding energies were corrected by referring to C1s peak at 284.6 eV, which contaminated the sample inadvertely. The $Cu_{2p3/2}$ binding

energy(932.7 eV) of fresh catalyst confirmed the reduced copper state. CuO also distinguishes itself from Cu_2O and Cu by having a shake-up peak. However, it is difficult to differentiate the oxidation sate of copper in sulfide species. The $Ce_{3d5/2}$ binding energies of both fresh and used catalysts are consistent with literature data for CeO_2. Two O_{1s} peaks were found in the XPS of the used catalyst while only the peak at lower binding energy was found on the fresh one. The peak of higher binding energy can be assigned to sulfate or carbonate, while the peak of low binding energy is assigned to metal oxide. Similarly, double S_{2p} XPS peaks were found on the used catalyst. The metal sulfate and sulfide contribute to the high and low binding energies, respectively. The sulfide peak is a major peak.

The quantitative surface compositional analysis of the $Cu_{0.15}Ce_{0.85}(La)O_x$ catalyst by XPS is given in Table 2. The results indicate that the surface was enriched in copper after use. The Cu/Ce and S/Cu ratios decreased by sputtering the surface with argon ion. But, the S/Cu ratio did not reach a zero value, which is considered to be due to the interference from the catalyst pores rather than sulfur diffusion in the bulk.

Reaction Mechanism

Previous studies have suggested that the reduction of sulfur dioxide by carbon monoxide on ceria proceeds via a redox mechanism[2].

$$\text{Cat-O} + \text{CO} \rightarrow \text{Cat-[ ]} + CO_2 \quad (1)$$

$$\text{Cat-[ ]} + SO_2 \rightarrow \text{Cat-O} + \text{SO} \quad (2)$$

$$\text{Cat-[ ]} + \text{SO} \rightarrow \text{Cat-O} + \text{S} \quad (3)$$

Creation of oxygen vacancies on the surface is a key step. The introduction of transition metals may provide surface sites for CO adsorption and facilitate the reduction of the fluorite oxide surface through strong metal-support interaction as found in the Pt-CeO_2[3] system.

$$\text{Cat-M---CO} + \text{Cat-O} \rightarrow \text{Cat-M} + \text{Cat-[\ ]} + CO_2 \quad (4)$$

$$\text{Cat-M} + S_X \rightarrow \text{Cat-}MS_X \quad (5)$$

$$\text{Cat-}MS_X + CO \rightarrow \text{Cat-M} + COS \quad (6)$$

However, the transition metal can be sulfided by the elemental sulfur product through reaction 5. Thus, the adsorbed CO on catalyst surface can pick up oxygen(reaction 1) and sulfur(reaction 6). COS formation thus becomes the result of these two competitive processes. COS formation prevails in following two cases. When excess CO exists or the oxidant is not sufficient, the extra CO reacts with elemental sulfur to form COS. When the oxygen is more strongly bound than sulfur, the adsorbed CO picks up sulfur to form COS. This reasoning is evidenced by the COS evolution profiles(Figure 7 and 8) during catalyst activation and CO flushing of a used catalyst, respectively. In Figure 7, COS formation was dominant when the catalyst was not activated, decreasing to zero at fully activated state, while a small amount of COS was formed at a later reaction time. The latter must be the result of reaction of a small amount of CO with sulfur on the catalyst surface. The COS evolution profile shown in Figure 8 resulted from the reaction of CO and residual sulfur on the surface during 2% CO/He scavenging of the used catalysts following a helium flush. A simple exponential decay of COS(t) predicted by assuming a formation rate $r_{COS}=k_S[S]_{surface}P_{CO}$ fits well the experimental data.

CONCLUSION

Strong interaction of ceria and copper contributes to the catalytic activity enhancement for the Cu-Ce-O system. The copper in finely dispersed state rather than in solid solution may benefit the catalytic performance. The Cu-Ce-O composite was enriched in copper on the surface and some of the surface

copper was converted to sulfide after use. Increasing copper content may result in high surface coverage(large copper particles) and decrease the strong interaction of ceria and copper. This may also favor the formation of undersirable by product COS. Further characterization of this catalyst system by surface analysis and the probe reaction($CO+O_2$) will be reported next quarter.

]Reference

1 C.D.Wagner, W.M. Rigg, L.E.Davis, J.F.Moulder and G.E. Muilenberg, Handbook of X-ray Photoelectron Spectroscopy, Perkin-Elmer Corporation, 1978.

2 W.Liu, M. Flytzani-Stephanopoulos and A. F. Sarofim DOE, Quarterly Technical Report No. 4, 1993

3 H.C.Yao and Y.F.Y. Yao, J. Catal., 86(1984)254-265.

Table 1

Binding Energies of Elements in the $Cu_{0.15}Ce_{0.85}(La)O_x$ Catalyst Determined by ESCA MULTIPLEX(mg, 300 W)

element	fresh(eV)	used(eV)	note[a]
$Cu_{2p3/2}$	932.7	932.4	Cu, Cu_2O copper sulfide
$Ce_{3d5/2}$	881.9	882.4	CeO_2
O_{1s}	529.0	529.3(72%)	metal oxide(CeO_2)
		531.7(28%)	metal sulfate, carbonate
S_{2p}	-	162.6(74%)	copper sulfide
		168.0(26%)	metal sulfate

a: assignment primarily based on the data in Wagner, C.D. et al.(eds.), Handbook of X-ray Photoelectron Spectroscopy[1].

Table 2

Surface Compositional Analysis of $Cu_{0.15}Ce_{0.85}(La)O_x$ Catalyst by XPS

Atomic ratio	Cu/Ce	S/Cu
bulk material[a]	0.176	0
fresh catalyst surface	0.133	0
used catalyst		
initial surface	0.364	1.59
1-min Ar^+ sputtering	0.206	1.36
7-min Ar^+ sputtering	0.151	1.15

a: based on stoichiometry.

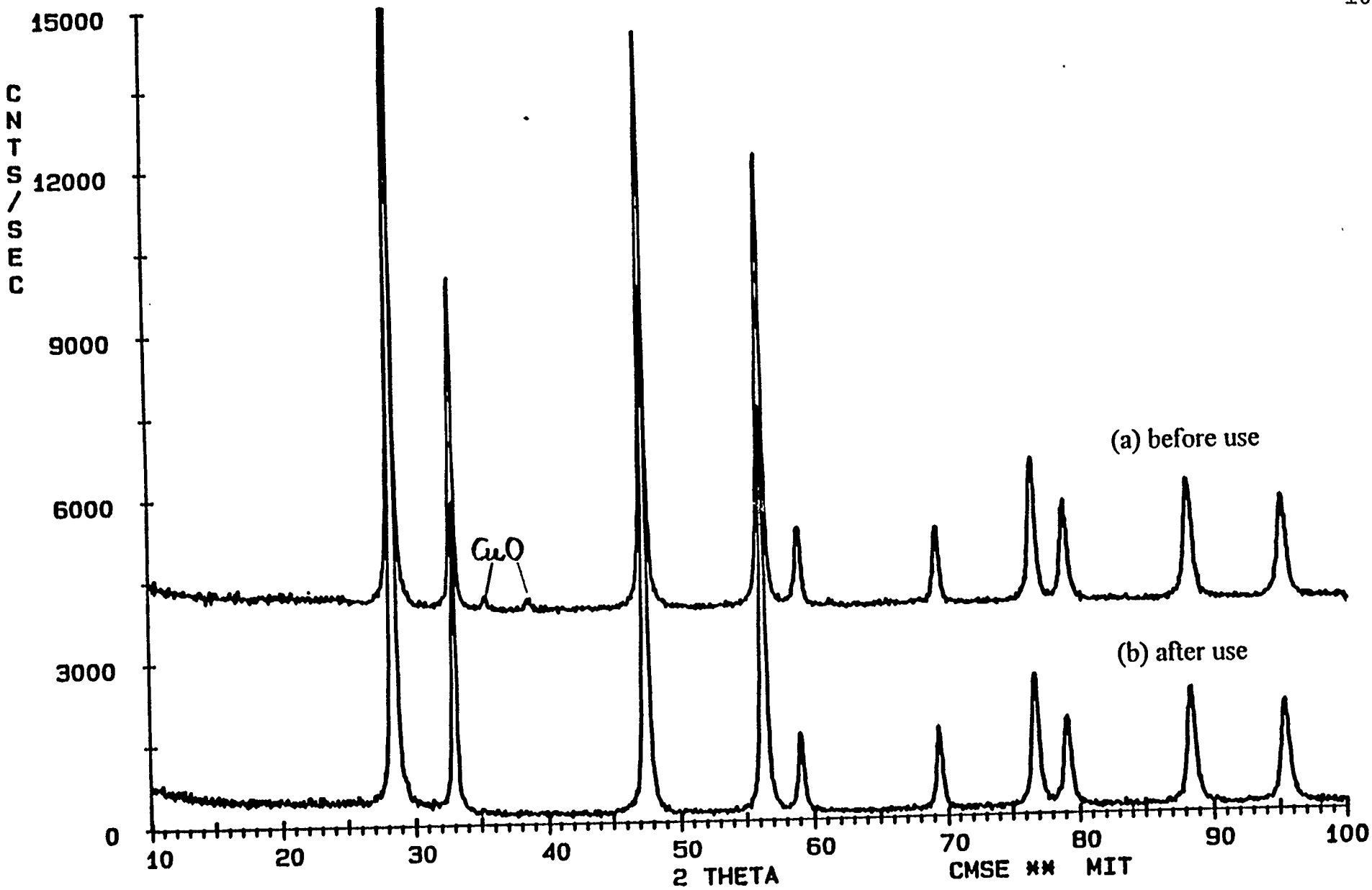

Figure 1. X-ray Diffractograms of the 3.7% Cu/CeO2 Catalyst.

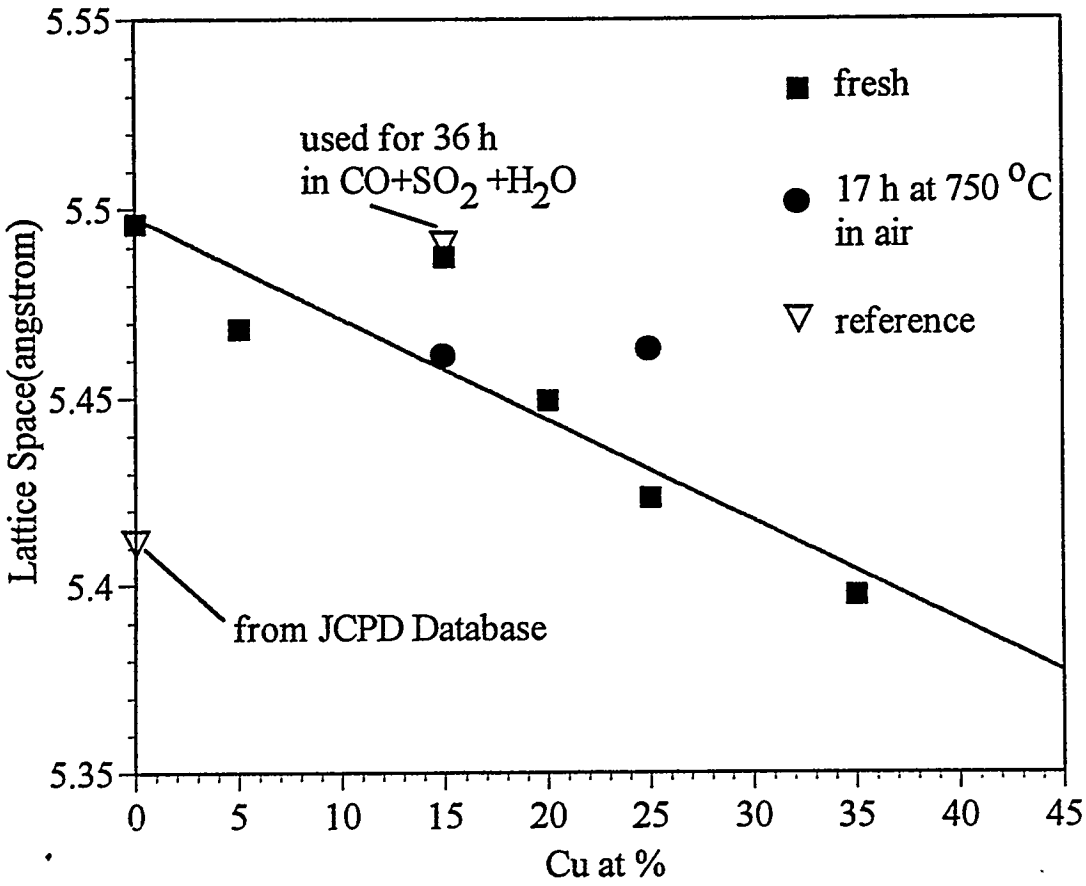

Figure 2. Variation of Lattice Parameter of CeO_2 with Copper Content and Thermal Treatment

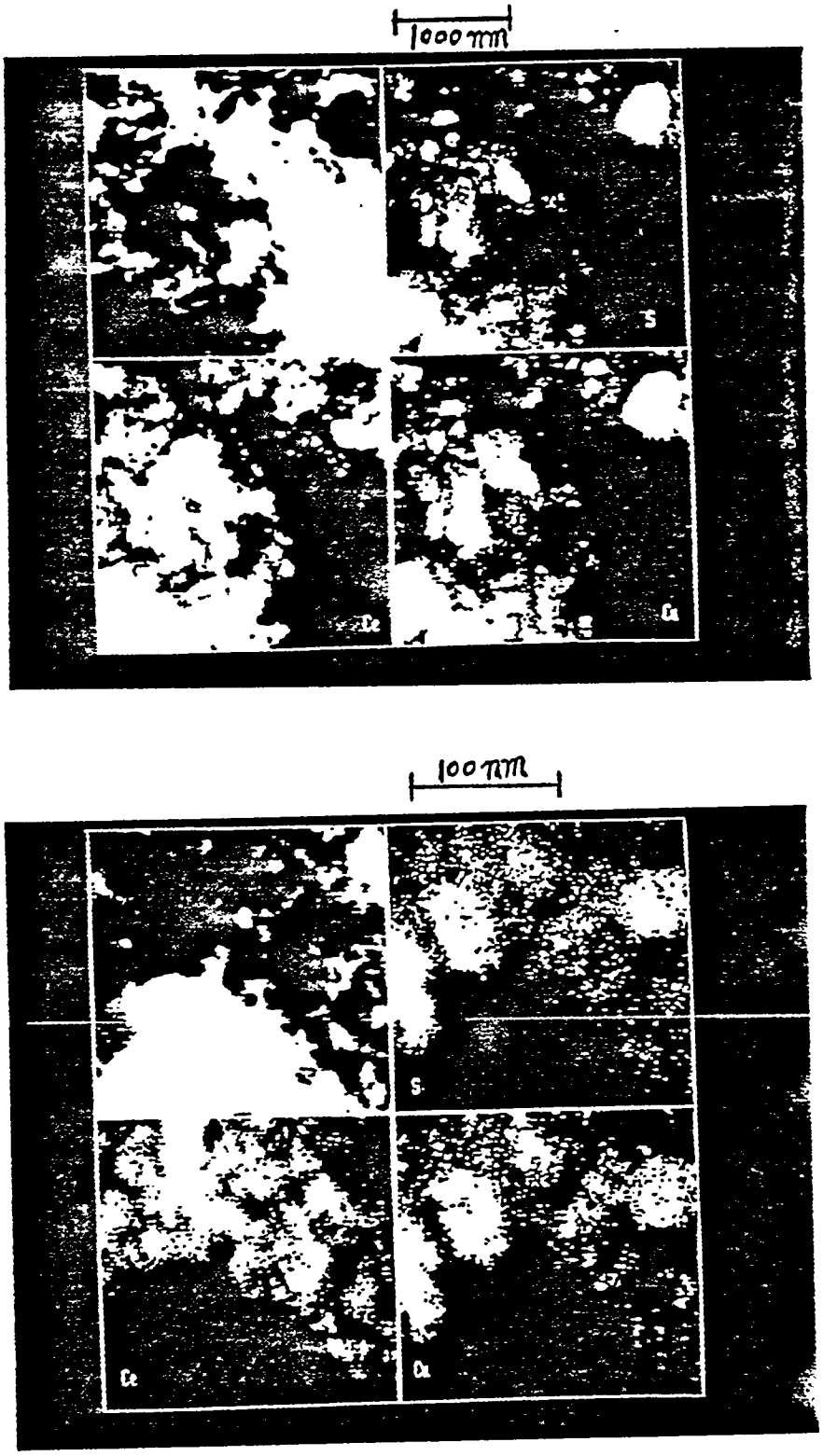

Figure 3. STEM Elemental Mapping of the Used Cu0.2Ce(La)0.8Ox Catalyst.

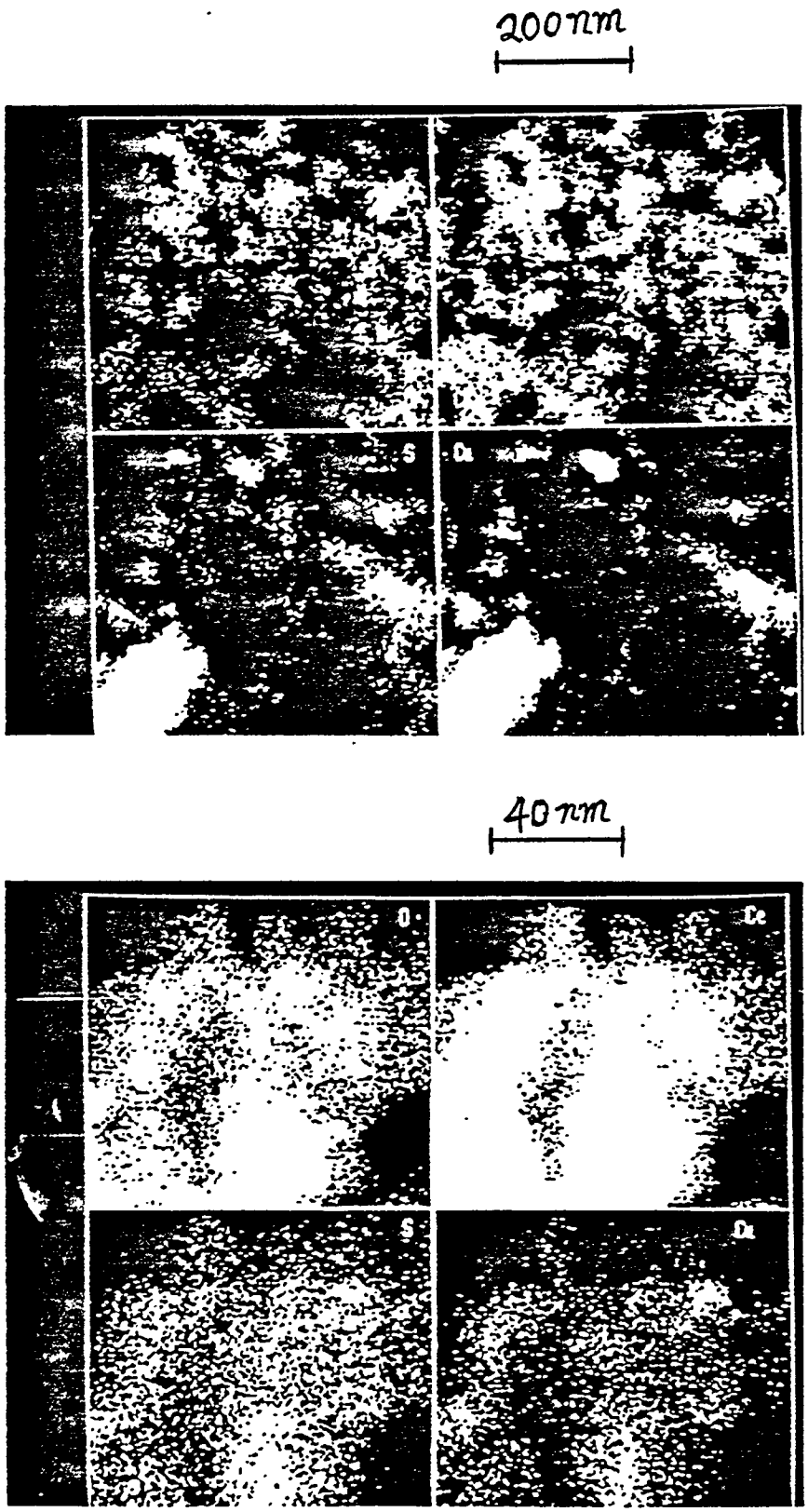

Figure 4. STEM Elemental Mapping of the Used Cu0.15Ce(La)0.85Ox Catalyst.

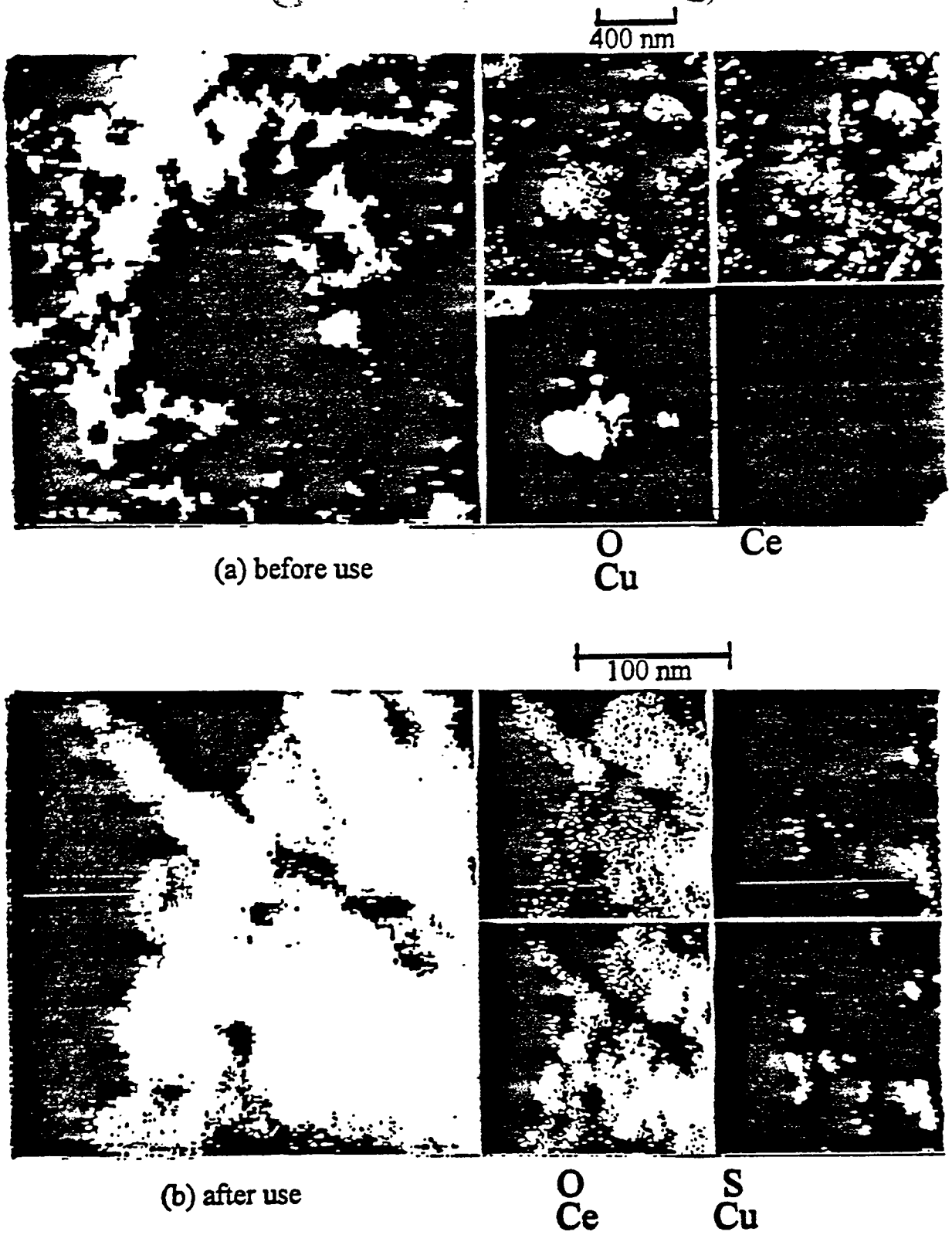

Figure 5. STEM Elemental Mapping of the 3.7% Cu/CeO2 Catalyst.

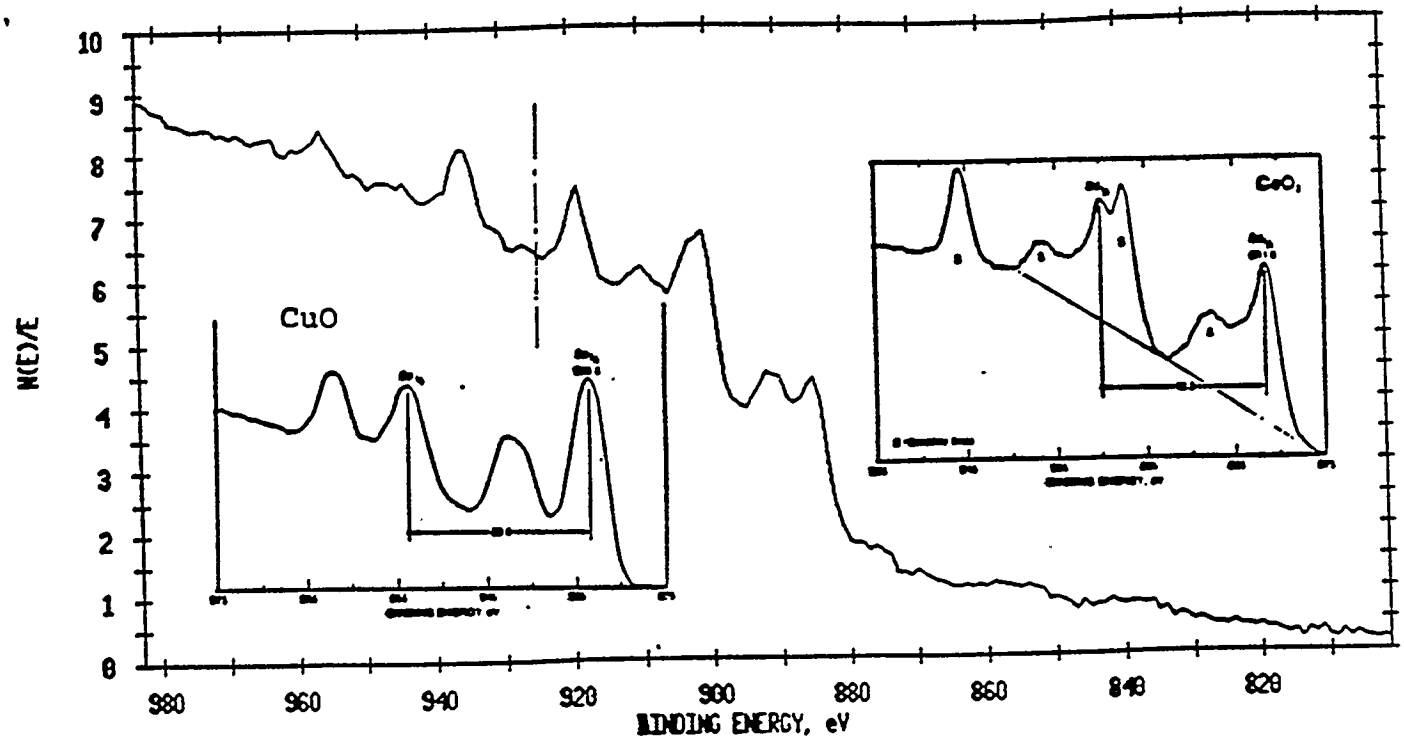

(a)

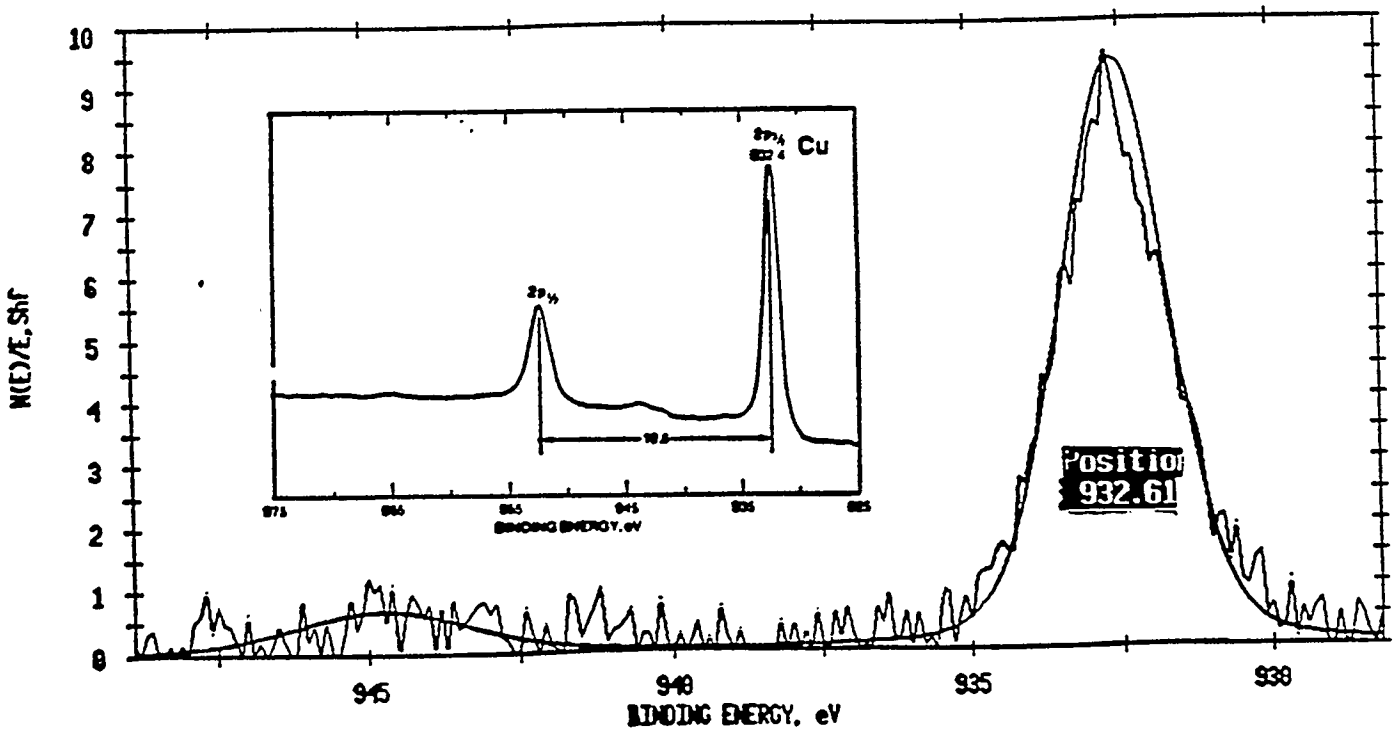

(b)

Figure 6. XPS of Fresh Cu0.15Ce(La)0.85Ox Catalyst(mg, 300 w)
(a) Survey.(b) Multiplex.

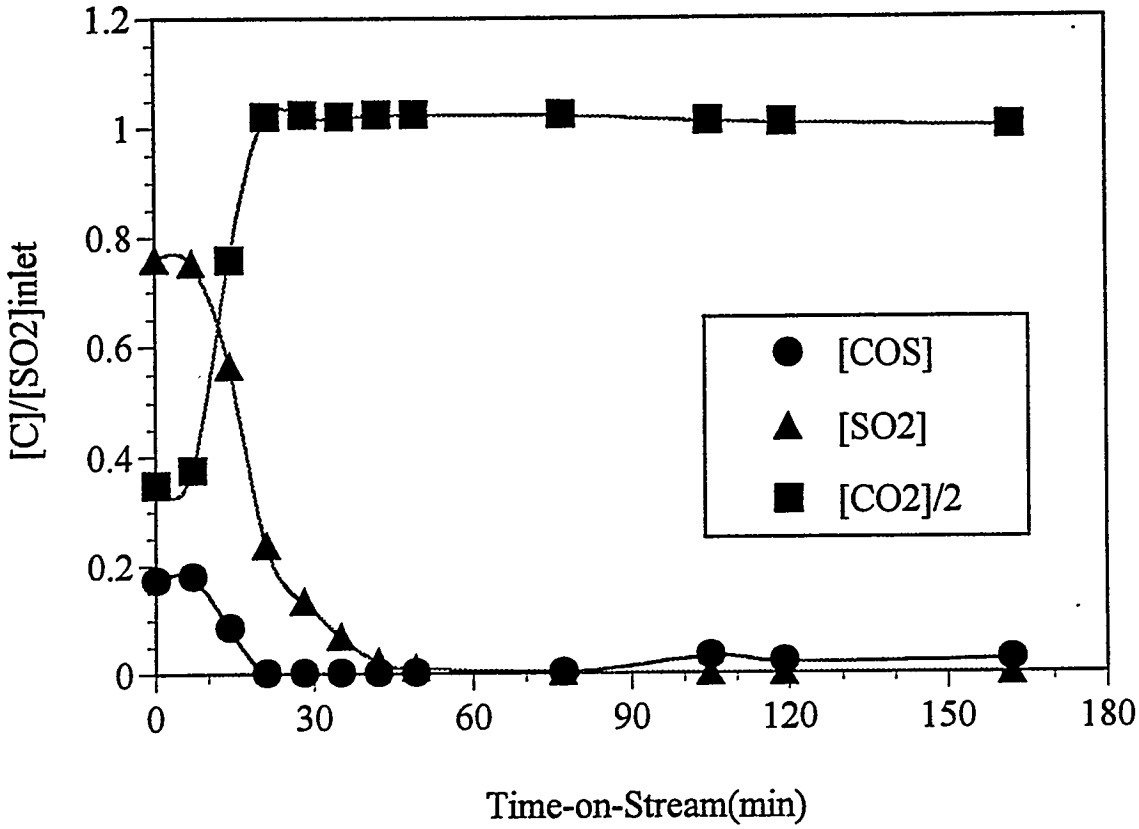

Figure 7. Activation Profile of $Cu_{0.15}Ce(La)_{0.85}O_x$ Catalyst at 510 ^{o}C(1% SO_2, 2.06% CO).

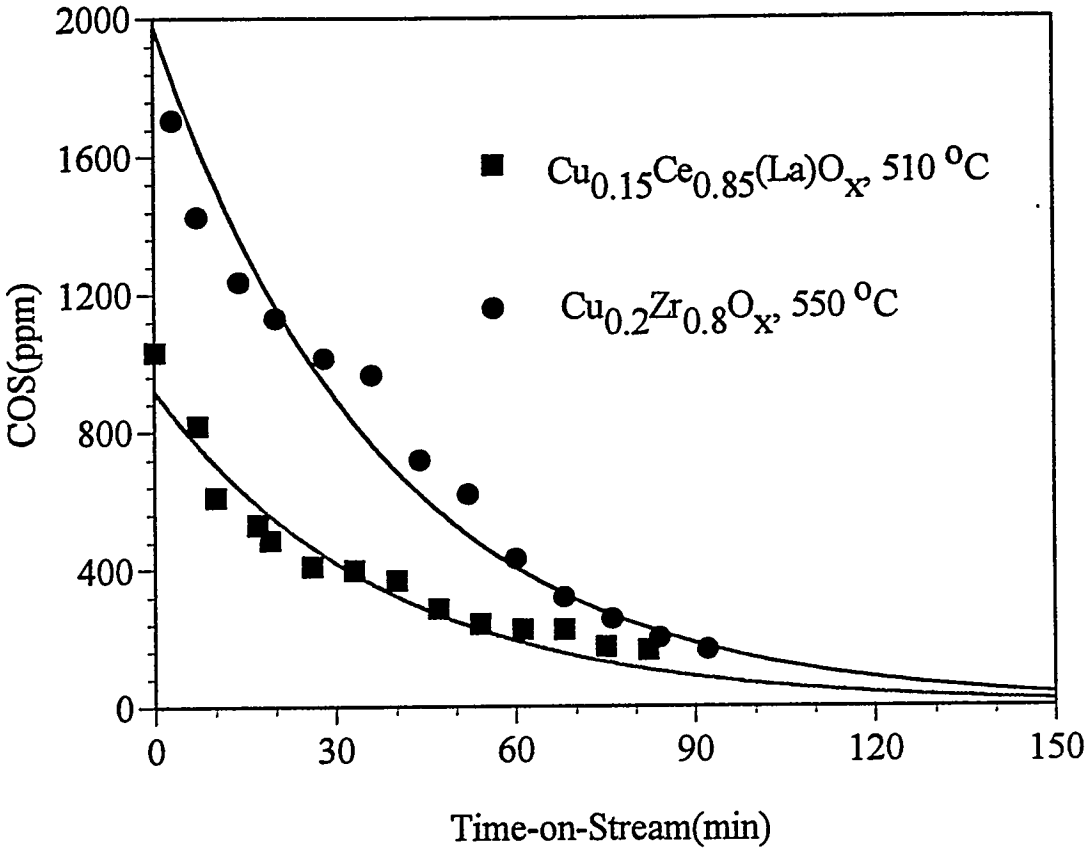

Figure 8. COS Evolution Profile During 2% CO/He Scavenging of Spent Catalyst.